Numerical simulation of large strain fracture problems using X-FEM

Grégory Legrain, Erwan Verron, Nicolas Moës

Numerical simulation of large strain fracture problems using X-FEM

G. Legrain, E. Verron & N. Moës
GeM – Institut de Recherche en Genie Civil et Mecanique, Nantes, France

ABSTRACT: Fracture of rubber-like materials is still an open problem. Indeed, it deals with issues related to the fracture itself (crack growth law, stress singularity around the crack tip), and also issues related to the bulk material behaviour (non-linear elasticity, large strain, incompressibility). The present study focuses on the application of the eXtended Finite Element Method (X-FEM) to the large strain fracture mechanics, under plane stress conditions. Two important aspects of this problem are investigated: the formulation used to solve the problem and the determination of suitable enrichment functions. The method is compared with Abaqus to demonstrate its robustness and capabilities for large strain problems.

1 INTRODUCTION

Fracture of rubber-like materials is still an open problem, as pointed out in (Charrier, Kuczynski, Verron, Marckmann, Gornet, and Chagnon 2003). Indeed, very few tools exist to solve this particular kind of problems. They cannot avoid the remeshing issue coming from crack growth, which for some of them must be handled by the user at each step of propagation. These problems contrast with linear fracture mechanics, where simulation tools have improved over the past years. New tools has been developed like meshless methods (EFGM (Lu, Belytschko, and Gu 1994) or HP-clouds (Duarte and Oden 1996)) to avoid the meshing of the domain studied, and by enriching the approximation basis. Finite element methods have also been modified within the partition of unity framework (Babuska and Y. Melenk 1997). One of these methods based on the partition of unity is the eXtended Finite Element Method. This method was first proposed as a response to the remeshing issue in crack propagation in linear fracture mechanics (Belytschko and Black 1999) (Moës, Dolbow, and Belytschko 1999). The eXtended Finite Element Methoduses the Partition of Unity in two ways: first to take into account the displacement jump across the crack faces far away from the crack tip, but also to enrich the approximation close to the tip with some knowledge of asymptotic fields. This method exhibits advantages which are in common with meshless methods (enrichment of the interpolation basis) and with Finite Element methods (mesh based approximations). A lot of linear fracture mechanics applications have been solved with the X-FEM approach: crack growth with friction (Dolbow, Moës, and Belytschko 2001), arbitrary branched and intersecting cracks (Daux, Moës, Dolbow, Sukumar, and Belytschko 2000), three dimensional crack propagation (Moës, Gravouil, and Belytschko 2002; Gravouil, Moës, and Belytschko 2002). The method has also been coupled with the level set approach (Sethian 1996) (Stolarska, Chopp, Moës, and Belytschko 2001a) for greater robustness and versatility. The main purpose of this paper is to show how to solve nonlinear fracture mechanics problem with the eXtended Finite Element Method, in particular for rubber-like material. It seems that only one paper has been published on this problem. This study, presented by Dolbow and Devan (Dolbow and Devan 2004) is about geometrically nonlinear fracture with the eXtended Finite Element Method, but more precisely about the locking issue occurring in plane strain analysis. The present paper will focus on the enrichment around the crack tip in nonlinear fracture mechanics, and will show the robustness and versatility of the eXtended Finite Element Method approach.

Nonlinear fracture mechanics study for rubber-like material really started in the 1950's with Rivlin and Thomas (Rivlin and Thomas 1953), who showed that the fracture of rubber was controlled by one parameter: the tearing energy. This parameter is equivalent to the energy release rate, and thus to the J-Integral. They also introduced a parameter (k) which relies the tearing energy with the strain energy density in the testpiece. They also argued that this parameter should only depend on the elongation. A lot of experiments has been done by Rivlin & Thomas, but also by Greensmith (Greensmith 1963) to obtain formulas describing this factor. On the other hand, Lake (Lake 1970) proposed an energetic way to approximate it, and more recently, O.H. Yeoh (Yeoh 2002) used a method based on crack

surface displacement to model k, and confronted it with finite element simulations. This paper is organized as follows: In the next section, we will discuss the governing equations of the problem. Then, we will present technical aspects of the implementation of the eXtended Finite Element Methodto nonlinear elasticity, before following with numerical examples of this implementation. Finally, we will conclude on the results presented, and present possible extensions to this work.

2 GOVERNING EQUATIONS

2.1 *Deformation of a cracked body in large strain*

Consider a thin cracked sheet $\mathcal{B}$ defined by its mid-plane surface Ω and its thickness distribution H in the reference undeformed configuration ($\mathcal{C}_0$). Under plane mechanical loading, B deforms and occupies the configuration ($\mathcal{C}$). The corresponding mid-plane surface, boundary and thickness distribution are respectively denoted ω, $\partial\omega$ and h. Figure 1 presents the notations. The motion between ($\mathcal{C}_0$) and ($\mathcal{C}$) can be described by the mapping ϕ which relates the current position of a particle, $\mathbf{x}$, at time t, to its initial position $\mathbf{X}$:

$$\mathbf{x} = \phi(\mathbf{X}, t) \tag{1}$$

In the deformed configuration, the boundary of $\mathcal{B}$ can be split into 2 disjoined parts: $\partial\omega_u$ on which the displacement field is enforced (Dirichlet boundary condition), and $\varpi\omega_T$ on which the surface traction is enforced (Neumann boundary condition). More precisely, $\varpi\omega_T$ includes the crack faces $\varpi\gamma_{C1}$ and $\varpi\gamma_{C2}$. The corresponding parts of the boundaries in the reference configuration are denoted by $\varpi\Omega_u$ (Dirichlet boundary condition), and by $\varpi\Omega_T$ (Neumann boundary condition), and by $\varpi\Gamma c_1$ and $\varpi\Gamma c_2$ for the two crack faces. Mathematically, these crack boundaries are different because of the bijectivity of the mapping ϕ even if they are superimposed in ($\mathcal{C}_0$), as shown in Fig. 1. Considering that there is no body forces, the material description of strong form of the boundary value problems is:

$$\begin{array}{ll} Div_{\mathbf{X}}\, \underline{\underline{P}} = \mathbf{0} & in\ \Omega \\ \mathbf{u}(\mathbf{x}) = \mathbf{u_d} & on\ \partial\Omega_u \\ \underline{\underline{P}} \cdot \mathbf{N} = \mathbf{T_d} & on\ \partial\Omega_t \setminus ((\partial\Gamma_{C1}) \cup (\partial\Gamma_{C2})) \\ \underline{\underline{P}} \cdot \mathbf{N} = \mathbf{0} & on\ \partial\Gamma_{C1}\ and\ \partial\Gamma_{C2} \end{array} \tag{2}$$

In these equations $\underline{\underline{P}}$ is the first Piola-Kirchhoff stress tensor, $\mathbf{u}$ is the displacement field, $\mathbf{u_d}$ is the prescribed displacement field, $\mathbf{N}$ stands for the unit exterior vector normal to the boundary $\partial\Omega_T$ and $\mathbf{T_d}$ is the prescribed Piola-Kirchhoff traction vector, i.e. the force measured per unit reference boundary length. According to

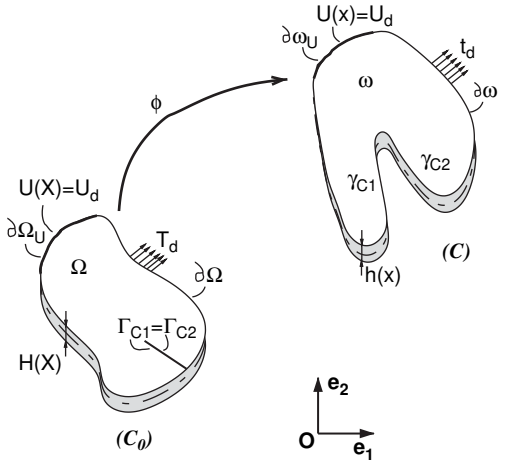

Figure 1. Notations of the model problem.

these equations, the Principle of Virtual Work in the material description is expressed as:

$$\begin{aligned} \mathcal{F}(\mathbf{u}, \delta\mathbf{u}) &= \int_\Omega H(X)\, \underline{\underline{S}} : \delta\underline{\underline{E}} d\Omega \\ &- \int_{\partial\Gamma_T} \mathbf{T_d} \cdot \delta\mathbf{u}\, d\Gamma = 0 \quad \forall\delta\mathbf{u} \end{aligned} \tag{3}$$

in which $\underline{\underline{S}}$ is the second Piola-Kirchhoff stress tensor, $\underline{\underline{E}}$ the Green-Lagrange strain tensor and $\delta\mathbf{u}$ represents the virtual displacement field. In the case of rubber-like materials, the above equation is highly nonlinear (due to both large strain and material nonlinearities). Its linearization is an essential prerequisite for the use of a Newton-like algorithm:

$$\begin{aligned} D\mathcal{F}(\mathbf{u}, \delta\mathbf{u})[\mathbf{u}] &= \int_\Omega H\ D\underline{\underline{E}}[\delta\mathbf{u}] : \underline{\underline{\underline{\underline{\mathcal{C}}}}} : D\underline{\underline{E}}[\mathbf{u}]\ dV \\ &+ \int_\Omega H\, \underline{\underline{S}} : \left[(Grad_X \mathbf{u})^T \cdot (Grad_X \delta\mathbf{u}) \right]\ dV \end{aligned} \tag{4}$$

where $D\underline{\underline{\mathcal{F}}}$ is the directional derivative operator and $\underline{\underline{\underline{\underline{\mathcal{C}}}}}$ is the *material elasticity tensor*. Here, the prescribed tractions were supposed not to depend on the displacement field. Finally, the constitutive equation of the material is examined. The material is supposed homogeneous, isotropic and incompressible. Moreover the general theory of hyperelasticity is considered. Here the material is assumed to obey the Neo-Hookean constitutive equation. The corresponding strain energy function is:

$$W = \frac{\mu}{2}(Tr(\underline{\underline{C}}) - 3) \tag{5}$$

where μ is the shear modulus and $\underline{\underline{C}}$ stands for the right Cauchy-Green dilatation tensor ($\underline{\underline{C}} = \underline{\underline{I}} + 2\underline{\underline{E}}$). The second Piola-Kirchhoff stress tensor is given by:

$$\underline{\underline{S}} = 2\frac{\partial W}{\partial C} - p\underline{\underline{C}}^{-1} = \mu\underline{\underline{I}} - p\underline{\underline{C}}^{-1} \tag{6}$$

In this equation p is the hydrostatic pressure due to the incompressibility of the material, it is determined using equilibrium equations. Because of small thickness of the sheet and plane loading, plane stress assumption is made. In this case, the thickness direction is irrelevant and the thickness variation is simply given by:

$$h^2 = \frac{H^2}{det(\bar{\underline{\underline{C}}})} \tag{7}$$

where $\bar{\underline{\underline{C}}}$ is the in-plane dilatation tensor. As a consequence, the hydrostatic pressure can explicitly be evaluated and the in-plane second Piola-Kirchhoff stress tensor is:

$$\bar{\underline{\underline{S}}} = \mu\left[\bar{\underline{\underline{I}}} - det(\bar{\underline{\underline{C}}})^{-1}\bar{\underline{\underline{C}}}^{-1}\right] \tag{8}$$

where $\bar{\underline{\underline{I}}}$ is the 2×2 identity tensor. Finally the 4th order elasticity tensor $\underline{\underline{\underline{\underline{C}}}}$ of Eq. (4) reduces to:

$$\underline{\underline{\underline{\underline{C}}}} = 2\mu\, det(\bar{C})^{-1}\left(\bar{\underline{\underline{C}}}^{-1} \otimes \bar{\underline{\underline{C}}}^{-1} + \underline{\underline{\underline{\underline{\mathcal{I}}}}}\right) \tag{9}$$

where $\underline{\underline{\underline{\underline{\mathcal{I}}}}} = \partial\bar{\underline{\underline{C}}}^{-1}/\partial\bar{\underline{\underline{C}}}^{-1}$.

3 DISCRETIZATION BY THE X-FEM

The formulation used in this study will be the total Lagrangian formulation, as discussed later. Thus we will have to approximate the displacement over the initial configuration. In classical finite elements, the approximation of a vectorial field $\mathbf{u}(\mathbf{X})$ on an element Ω_e is written as:

$$\mathbf{u}(\mathbf{X})|_{\Omega_e} = \sum_{i=1}^{Nddl\_e} u^i\, \mathbf{N^i} \tag{10}$$

Here within the partition of unity framework, the approximation is enriched as:

$$\mathbf{u}(\mathbf{X})|_{\Omega_e} = \sum_{i=1}^{Nddl\_e} \mathbf{N^i}\left(u^i + \sum_{j=1}^{Nenr} a_j^i\, \phi_j(\mathbf{X})\right) \tag{11}$$

Where Nddl_e is the number of degrees of freedom of the element, Nenr the number of additional degree of freedom, a_j^i the additional dof associated to dof i and ϕ_j the *jth* scalar enrichment function. *Remarks:*

- As we can see, additional dofs have been added to the finite element model. Thus, we won't know *a priori* the exact number of dofs of the structure.
- The approximation on every elements (11) can be assembled on the whole structure to obtain an approximation of $\mathbf{u}(\mathbf{X})$ on the entire domain Ω.
- Classically, a dof will be enriched if its associated nodal support contains the discontinuity (crack here) (Moës, Dolbow, and Belytschko 1999).

Two different types of enrichment are used in fracture mechanics (see (Moës, Dolbow, and Belytschko 1999)):

- A discontinuous enrichment for nodes whose support is bisected by the crack. In this case, the interpolation of the displacement field must be discontinuous across the crack. An Heaviside jump function is used to model this discontinuity: this function is equal to $+1$ on one side of the crack, and -1 on the other side. The associated dof will manage the magnitude of this displacement discontinuity. The Heaviside function is computed using the levelset representation of the crack (Stolarska, Chopp, Moës, and Belytschko 2001b).
- A near tip enrichment for nodes whose support contains the crack tip. In linear fracture mechanics, the enrichment functions are based on the asymptotic displacement field near the tip of the crack. The problem in nonlinear elasticity is to find this asymptotic field. The determination of this field will be discussed in the next part.

As a remark, we can see that there are gradient discontinuities inside enriched elements. That's why all the elements containing the discontinuity are partitioned into sub-elements (Moës, Dolbow, and Belytschko 1999). Note that no additional degrees of freedom are associated with these sub-elements.

3.1 *Near-tip enrichment*

As pointed out above, the choice of the right enrichment function is fundamental in the eXtended Finite Element Method in order to achieve precision, even with coarse meshes. The choice of those functions is now discussed. Suitable enrichment functions are related to the asymptotic displacement field around the crack tip. The determination of this field is a complex topic since the problem is highly nonlinear. The oretical results were established in the incompressible plane stress case by Geubelle and Knauss (Geubelle and Knauss 1994a; Geubelle and Knauss 1994b; Geubelle and Knauss 1994c), in the general plane

strain case by Knowles and Sternberg (Knowles and Sternberg 1973; Knowles and Sternberg 1974) and in the incompressible plane strain case by Stephenson (Stephenson 1982). These studies were conducted using the generalized Neo-Hookean strain energy: Recall that in the present case, the incompressible plane stress assumption is adopted and the classical Neo-Hookean material is considered. Thus, the corresponding asymptotic field is given by (Geubelle and Knauss 1994a):

$$\begin{cases} v_1(r,\theta) \approx r\cos(\theta) \\ v_2(r,\theta) = r^{1/2}\sin(\theta/2) \end{cases} \tag{12}$$

where the v_1 and v_2 are the displacement projected respectively on E_1 and E_2 (see Fig. 2). Moreover, if second order terms are needed, it can be proved that only one additional term appears along the second axis. However, this term is defined by an implicit equation, thus it is not straightforward to use it numerically as enrichment. Finally the enrichment functions that will be used in the following is:

$$\phi = \left\{ r^{1/2}\ \sin(\theta/2) \right\} \tag{13}$$

As a comparison, in linear fracture mechanics, the enrichment functions are:

$$\phi \ = \ \left\{ r^{1/2}\sin(\theta/2), r^{1/2}\cos(\theta/2) \right. \tag{14}$$

$$\left., r^{1/2}\sin(\theta/2)\sin(\theta), r^{1/2}\cos(\theta/2)\sin(\theta) \right\}$$

The first term in (13) is similar to the only discontinuous term of Eq. (14). Moreover, it should be noted that the second term of Eq. (13) reduces to 'x' when expressed in the crack font coordinate system. This function being linear, it is already contained in the polynomial approximation space. The use of this function as an enrichment would lead to a ill-conditioned tangent matrix.

3.2 *Solving procedure*

We may now justify why the total Lagrangian formulation is used. The main reason stems from the method itself: The eXtended Finite Element Method, like classical finite element method defines a mapping between parent element and current element (using reference element as a step) (Cf Fig. 3) In an updated Lagrangian approach, the weak form is integrated on the last computed configuration, whereas in a total Lagrangian approach, the integration takes place on the reference configuration. The key problem is to know if the inverse mapping from current and/or reference element to parent element is possible. In classical linear FE, all the mapping involved are linear. So, both total or updated Lagrangian formulation will be possible. With X-FEM, the mapping between reference

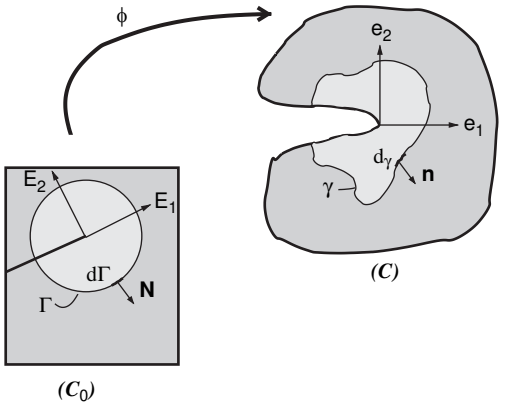

Figure 2. Deformation of a cracked body.

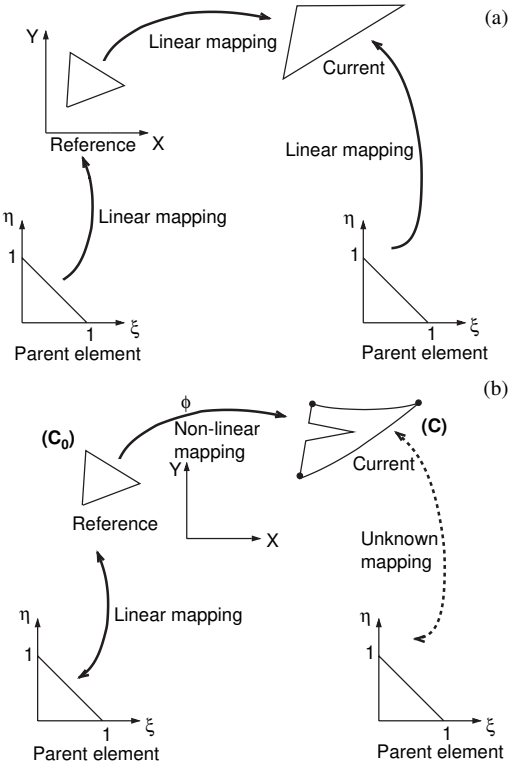

Figure 3. (a) Mappings associated to linear finite element, (b) Mappings associated to the eXtended Finite Element Method.

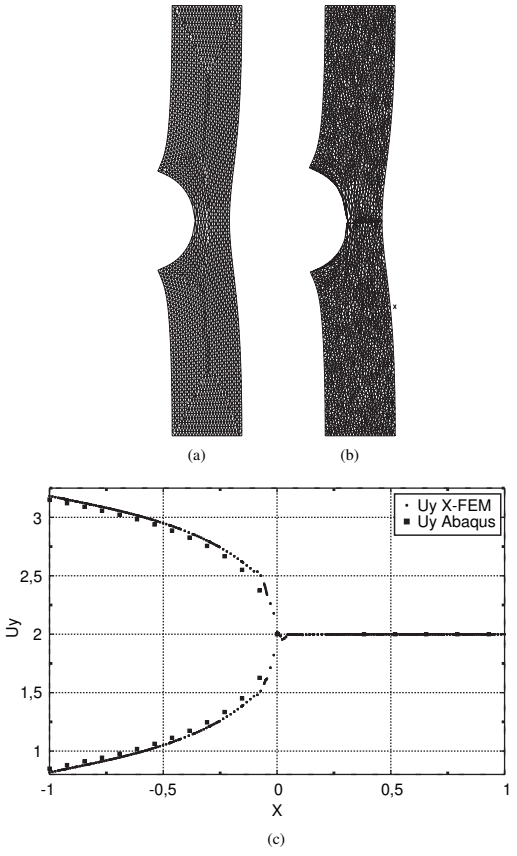

Figure 4. (a) Abaqus deformed configuration; (b) X-FEM deformed configuration; (c) Comparison of the two crack vertical displacements.

and actual configuration (as for actual – parent mapping) are nonlinear. Inverse mapping between these configurations cannot be obtained because of this nonlinearity. On the contrary, the mapping between parent and reference element remains linear. The total Lagrangian formulation will therefore be best fitted to the eXtended Finite Element Method. For more detailed explanations, see (Legrain, Moës, and Verron 2004). Since the total Lagrangian formulation is chosen, we will have to discretize the reference domain Ω, and interpolate the displacement field. The discretization of these equations is similar with discretization for classical finite element and becomes:

$$\left(K_{\alpha\beta}^{Phys} + K_{\alpha\beta}^{Geo}\right) du_\beta = f_\alpha^{int} - f_\alpha^{ext} \tag{15}$$

With K^{Phys} the physical tangent stiffness matrix, K^{Geo} the geometrical tangent stiffness matrix, $\mathbf{f}^{\mathbf{int}}$ the internal equivalent nodal forces, $\mathbf{f}^{\mathbf{ext}}$ the external equivalent nodal forces and **du** the correction to the current configuration. The expressions of these matrix and vectors are similar to finite element expressions.

4 NUMERICAL EXAMPLE

In this example, X-FEM and Abaqus (HKS) computation results are compared. A SET specimen (dimensions = 2 mm × 6 mm and crack length = 1 mm) is subjected to an enforced displacement of its top edge equal to 4 mm and its bottom edge is fixed. The material is Neo-Hookean with shear modulus $\mu = 0.4225$. The mesh used with Abaqus conforms to the crack surface and has the same element density as the X-FEM mesh which is unstructured (the crack runs through the elements). Deformed configurations are compared. Qualitatively, they are similar as shown in Figure 4(a) and (b). To compare them more precisely, the vertical displacement of the crack surface nodes versus their initial horizontal position are plotted in Figure 4(c). The deformed shape of the crack is very similar for the two simulations, and results obtained with X-FEM are reliable.

5 CONCLUSIONS

The application of the eXtended Finite Element Method to the field of high strain fracture analysis seems to be promising. Indeed, the numerical examples have shown the reliability of the method when dealing with high strain structural applications. More validations have been carried out in (Legrain, Moës, and Verron 2004) and have shown that high strain computation of the tearing energy was very accurate, even when dealing with coarse meshes or more complex loadings. However, the choice of the right enrichment functions may be a problem when dealing with more complex material behaviour, plane strain or three-dimensional analysis. This should be an important topic to investigate. One other important point is the enforcement of the incompressibility constraint. A first work has already been published on this topic (see (Dolbow and Devan 2004)), and may be a beginning.

REFERENCES

Babuska, I. and J.Y. Melenk (1997, February). The partition of unity finite element method. *International Journal for Numerical Methods in Engineering 40*(4), 727–758.

Belytschko, T. and T. Black (1999). Elastic crack growth in finite elements with minimal remeshing. *International Journal for Numerical Methods in Engineering 45*(5), 601–620.

Charrier, P., E. Kuczynski, E. Verron, G. Marckmann, L. Gornet, and G. Chagnon (2003). Theorical and numerical

limitations for the simulation of crack propagation in natural rubber components. In *Constitutive Models for Rubber III, Busfield & Muhr (eds)*.

Daux, C., N. Moës, J. Dolbow, N. Sukumar, and T. Belytschko (2000). Arbitrary branched and intersecting cracks with the eXtended Finite Element Method. *International Journal for Numerical Methods in Engineering 48*, 1741–1760.

Dolbow, J. and A. Devan (2004). Enrichment of enhanced assumed strain approximations for representing strong discontinuities: Addressing volumetric incompressibility and the discontinuous patch test. *International journal for numerical methods in engineering 59*, 47–67.

Dolbow, J., N. Moës, and T. Belytschko (2001). An extended finite element method for modeling crack growth with frictional contact. *Comp. Meth. in Applied Mech. and Engrg. 190*, 6825–6846.

Duarte, C. and J. Oden (1996). An hp meshless method. *Numerical methods for partial differential equations 12*, 673–705.

Geubelle, P. and W. Knauss (1994a). Finite strains at the tip of a crack in a sheet of hyperelastic material: I. homogeneous case. *Journal of Elasticity 35*, 61–98.

Geubelle, P. and W. Knauss (1994b). Finite strains at the tip of a crack in a sheet of hyperelastic material: Ii. special bimaterial case. *Journal of Elasticity 35*, 99–137.

Geubelle, P. and W. Knauss (1994c). Finite strains at the tip of a crack in a sheet of hyperelastic material: Iii. general bimaterial case. *Journal of Elasticity 35*, 139–174.

Gravouil, A., N. Moës, and T. Belytschko (2002). Non-planar 3d crack growth by the extended finite element and level sets. part II: level set update. *International Journal for Numerical Methods in Engineering 53*, 2569–2586.

Greensmith, H. (1963). Rupture of rubber part 10: The changes in stored energy on making a small cut in a test piece held in simple extension. *J. Appl. Polym. Sci. 7*, 993–1002.

HKS. *Abaqus/Standard user manual*. HKS.

Knowles, J. and E. Sternberg (1973). An asymptotic finite-deformation analysis of the elastostatic field near the tip of a crack. *Journal of Elasticity 3*, 67–107.

Knowles, J. and E. Sternberg (1974). Finite-deformation analysis of the elastostatic field near the tip of a crack: Reconsideration of higher order results. *Journal of Elasticity 4*, 201–233.

Lake, G. (1970). Application of fracture mechanics to failure in rubber articles, with particularly reference to groove cracking in tyres. In *Int. Conf. Yeld, Deformation and fracture of polymers, Cambridge*.

Legrain, G., N. Moës, and E. Verron (2004). Stress analysis around crack tips in finite strain problems using the extended finite element method. *International Journal for Numerical Methods in Engineering*, Accepted.

Lu, Y., T. Belytschko, and L. Gu (1994). Element-free galerkin methods. *International Journal for Numerical Methods in Engineering 51*, 221–258.

Moës, N., J. Dolbow, and T. Belytschko (1999). A finite element method for crack growth without remeshing. *International Journal for Numerical Methods in Engineering 46*, 131–150.

Moës, N., A. Gravouil, and T. Belytschko (2002). Non-planar 3D crack growth by the extended finite element and level sets. part I: Mechanical model. *International Journal for Numerical Methods in Engineering 53*, 2549–2568.

Rivlin, R. and A. Thomas (1953). Rupture of rubber. i. characteristic energy for tearing. *Journal for Polymer science 3*, 291–318.

Sethian, J. (1996). *Level Set Methods and Fast Marching Methods: Evolving Interfaces in Computational Geometry; Fluid Mechanics; Computer Vision; and Material Science*. Cambridge University Press.

Stephenson, R. (1982). The equilibrium field near the tip of a crack for finite plane strain of incompressible elastic materials. *Journal of Elasticity 12*, 65–99.

Stolarska, M., D. Chopp, N. Moës, and T. Belytschko (2001a). Modelling crack growth with level-set and the extended finite element method. *International Journal for numerical methods in Engineering 51*, 943–960.

Stolarska, M., D.L. Chopp, N. Moës, and T. Belytschko (2001b). Modelling crack growth by level sets and the extended finite element method. *International Journal for Numerical Methods in Engineering 51*(8), 943–960.

Yeoh, O. (2002). Relation between crack surface displacement and strain energy release rate in thin rubber sheets. *Mechanics of Materials 32*, 459–474.